Jurnal Teknologi

Full Paper

STUDIES OF THE KINETIC AND THERMODYNAMIC PARAMETERS OF LEVULINIC ACID IN THE CONVERSION TO ETHYL LEVULINATE VIA ESTERIFICATION CATALYSED BY SULFONATED FOOD WASTE CHAR

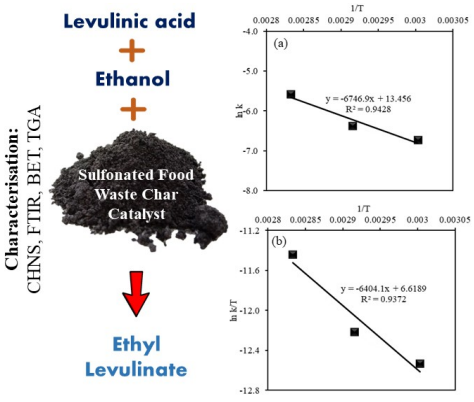
Hafis Adlan Rosmadi[a], Muzakkir Mohammad Zainol[a]*, Abdull Hafidz Hassan[a], Nur Aina Sakinah Salihuddin[a], Muhammad Ammir Ilham Azhar[a], Mohd Asmadi[b], Didi Dwi Anggoro[c], Ashraf Azmi[a], Noor Yahida Yahya[d], Zakariya Y. Mahssin[e], Norhidayah Abdul Hassan[e]

[a]Faculty of Chemical Engineering, Universiti Teknologi MARA, 40450 Shah Alam, Selangor, Malaysia
[b]Faculty of Chemical and Energy Engineering, Universiti Teknologi Malaysia, 81310 UTM Johor Bahru, Johor, Malaysia
[c]Department of Chemical Engineering, Diponegoro University, Semarang 50273, Indonesia St. Prof. Soedarto, SH, Tembalang, Semarang, Indonesia
[d]Faculty of Civil Engineering Technology, Universiti Malaysia Pahang Al-Sultan Abdullah, 26300 Gambang, Pahang, Malaysia
[e]Faculty of Civil Engineering, Universiti Teknologi Malaysia, 81310 UTM Johor Bahru, Johor, Malaysia

Article history
Received
21st June 2025
Received in revised form
13th November 2025
Accepted
19th November 2025
Published
1st November 2026

*Corresponding author
muzakkir@uitm.edu.my

Graphical abstract



Abstract

This work investigated the kinetics and thermodynamics of levulinic acid (LA) conversion to ethyl levulinate (EL) catalysed by sulfonated food waste char (SFC) catalyst. The food waste char was derived from the hydrothermal liquefaction of food waste that underwent sulfonation with sulphuric acid to prepare an acid-functionalised catalyst. The esterification reaction was performed by varying the process parameters, including catalyst particle size (300 and 600 µm), agitation speed (100 and 300 rpm), reaction time (1–4 h), and heating temperature (60–80 °C). The EL yield and LA conversion were determined through the concentration of the respective chemicals analysed by gas chromatography-mass spectrometry. Pseudo-homogeneous kinetic models were employed to determine the reaction order and kinetic parameters. Subsequently, the thermodynamic parameters were determined using the Eyring equation. Based on the results, the pseudo-first-order model was identified as the best-fit model to represent the reaction kinetics, yielding an activation energy of 56.1 kJ/mol, an enthalpy of activation of 52.3 kJ/mol, an entropy of activation of -190.9 J/mol·K, and a Gibbs free energy of activation of 84.4 kJ/mol.

Keywords: Ethyl levulinate, food waste, kinetic study, levulinic acid, thermodynamic study

DOI: https://doi.org/10.11113/jurnalteknologi.v89.25102

Abstrak

Kerja ini menyiasat kinetik dan termodinamik bagi penukaran asid levulinik (LA) kepada etil levulinat (EL) yang dimangkin oleh pemangkin arang sisa makanan tersulfonasi (SFC). Arang sisa makanan terhasil daripada pencairan hidroterma sisa makanan yang mengalami sulfonasi dengan asid sulfurik untuk menyediakan pemangkin berfungsi asid. Tindak balas pengesteran dilakukan dengan mempelbagaikan parameter proses, termasuk saiz zarah mangkin (300 dan 600 µm), kelajuan pengadukan (100 dan 300 rpm), masa tindak balas (1-4 jam), dan suhu pemanasan (60–80 °C). Hasil EL dan penukaran LA ditentukan melalui kepekatan bahan kimia masing-masing yang dianalisis oleh kromatografi gas-spektrometri jisim. Model kinetik pseudo-homogen digunakan untuk menentukan tertib tindak balas dan parameter kinetik. Selepas itu, parameter termodinamik tindak balas ditentukan menggunakan persamaan Eyring. Berdasarkan keputusan, model kinetik pseudo-tertib-pertama dikenal pasti sebagai model yang paling sesuai untuk mewakili kinetik tindak balas, memperoleh tenaga pengaktifan 56.1 kJ/mol, dengan entalpi pengaktifan 52.3 kJ/mol, entropi pengaktifan -190.9 J/mol·K, dan tenaga pengaktifan bebas Gibbs 84.4 kJ/mol.

Kata kunci: Etil levulinat, sisa makanan, kajian kinetik, asid levulinik, kajian termodinamik

© 202@ Penerbit UTM Press. All rights reserved

1.0 INTRODUCTION

Renewable carbon-based materials, such as lignocellulosic biomass, are generated from sources such as forests, agriculture, and plantations. Chemicals produced from biomass have added value as they contribute to sustainable chemistry [1]. One of these chemicals, which is levulinic acid (LA), has the potential to be synthesised from biomass, serving as a chemical precursor to produce alkyl levulinates [2]. The reaction of LA is carried out via esterification with alcohol to yield alkyl levulinates, owing to the significant advantages of levulinates as fuel additives and precursors for γ-valerolactone synthesis [3].

The synthesis of levulinates through LA esterification is considered one of the simplest and most sustainable routes to produce ethyl levulinate (EL), as the reaction produces only water as a by-product [4]. The esterification of LA involves the application of an acidic catalyst to increase the EL yield. Previously, homogeneous acid catalysts such as hydrochloric acid and sulphuric acid have been used in LA esterification [5]. However, heterogeneous or solid catalysts are the preferred option as they offer characteristics such as robust catalytic activity, stability, high reusability, and good practicality [1]. The use of homogeneous acid catalysts has led to corrosion of process equipment and environmental damage [6].

Progress has been made in converting biomass materials into heterogeneous catalysts to achieve high selectivity of levulinates. Heterogeneous solid catalysts are available in various types, such as carbon-based, silica-based, and zeolite-based catalysts, with each catalyst differing in terms of product yield [7]. One of the promising heterogeneous catalysts is sulfonated carbon [8, 9]. Sulfonated carbon-based catalysts possess a large surface area with microporous and mesoporous structures [10, 11]. Various materials can be used as carbon feedstock for preparing solid acid catalysts via sulfonation. For example, carbon catalysts can be produced from food waste through several procedures. Food waste is expected to reach 416 Mt by 2025, contributed by Asian countries [12], making it a potential feedstock for carbon-based catalysts.

Catalysts accelerate esterification by lowering the energy required for the chemical transformation to reach the transition state, thus reducing the activation energy (E_a) of the reaction [13]. However, reaction rates vary depending on the reactivity of the catalyst used and the reaction parameters [14]. This variation is due to the different activity of the catalyst used to achieve a high product yield at low reaction temperatures and short reaction times. Zainol et al. [15] found that the EL produced from the reaction of LA with ethanol catalysed by a carbon catalyst followed the pseudo-first-order kinetic model with an E_a of 20.2 kJ/mol. A previous study by Tiong et al. [16] reported that LA esterification catalysed by an indium trichloride-ionic liquid catalyst exhibited an E_a of 28.1 kJ/mol based on the fitted pseudo-first-order kinetic model. Yadav and Yadav [17] established a pseudo-first-order kinetic equation with an E_a of 37.7 kJ/mol for a similar reaction but catalysed by the UDCaT-5 catalyst.

This research focused on studying the kinetic and thermodynamic parameters for LA esterification to EL catalysed by sulfonated food waste char (SFC). A series of esterification reactions were conducted under various conditions and reaction parameters. The scope of the research includes investigating the effect

DOI: https://doi.org/10.11113/jurnalteknologi.v89.25102

of catalyst particle size, agitation speed, reaction time, and reaction temperature. Gas chromatography was employed to analyse the concentrations of EL and LA. The data were fitted to a mathematical model to determine the reaction kinetic parameters and were also applied to the Eyring equation to obtain the thermodynamic parameters.

2.0 METHODOLOGY

2.1 Material

Sulphuric acid (H_2SO_4, 95–97%, Supelco, USA) and food waste char from hydrothermal liquefaction (HTL) were used for the preparation of sulfonated char catalyst. Levulinic acid ($C_5H_8O_5$, 98%, Merck, Germany) and ethanol (C_2H_6O, 95%, Chemiz, Malaysia) were used for the esterification reaction, while ethyl levulinate ($C_7H_{12}O_3$, 99%, Merck, Germany) was utilised as a standard for the analysis of the synthesised EL from the reaction. The food waste char was obtained from the HTL studied by Mahssin et al. [12]. Simulated food waste of 2:1:2 (rice:vegetable:chicken) as feedstock was converted via HTL for a ratio of 40:100 (waste:water) at 225 °C and 1 h.

2.2 Preparation and Characterisation of Sulfonated Food Waste Char

The sulfonated char catalyst was prepared through the sulfonation of food waste char in an autoclave hydrothermal reactor. The sulfonated carbon-based catalyst effectively catalysed LA esterification, as reported by Hassan et al. [18]. Firstly, the char was preheated in a furnace, then sulfonated with a high concentration of H_2SO_4 at 180 °C for 6 h using hydrothermal carbonisation. The sulfonated char catalyst was then diluted with distilled water prior to filtration. The slurry was washed continuously and filtered using vacuum filtration. The washing-filtration steps were repeated until the filtrate reached a pH of approximately 6.8–7.0, and the SFC catalyst was then collected. The sample was dried in an air-circulation oven at 80 °C (overnight) to obtain the SFC catalyst for further use in the reaction.

The SFC catalyst was characterised by Fourier transform infrared (FTIR), thermogravimetric analysis (TGA), CHNS, and Brunauer-Emmett-Teller (BET) analysis. The presence of functional groups and chemical bonds was identified by FTIR spectroscopy with a Perkin Elmer Spectrum instrument using KBr pellets in the wavenumber range of 370–4000 cm^{-1}. The peaks of sulfonated char and preheated char were compared to identify changes in functional groups following sulfonation. Subsequently, the TGA/DSC 1 STAR System (METTLER TOLEDO) was used to assess the thermal stability and degradation of the sulfonated and preheated char by heating in the range of 30–900 °C at a heating rate of 10 °C/min under a nitrogen (N_2) atmosphere. The thermal stability and degradation peaks of the samples were observed based on the TG and DTG curves at different temperature ranges, respectively. In addition, the total surface area was determined based on the N_2 adsorption-desorption analysis via a Micromeritics 3-Flex instrument using the BET method. The sample was degassed under vacuum at 200 °C for 6 h prior to standard N_2 adsorption-desorption at -196 °C.

2.3 Ethyl Levulinate Synthesis and Product Analysis

Levulinic acid and ethanol were esterified in a reflux setup as a batch reactor for EL synthesis (Figure 1). Different particle sizes of SFC (300 and 600 µm) were employed to study the internal diffusion resistance of the reaction. Meanwhile, the external diffusion resistance was investigated using different agitation speeds of 100 and 300 rpm. The kinetic and thermodynamic parameters were examined through experiments conducted at a range of temperatures of 60–80 °C and reaction times of 1–4 h. Throughout the study, the molar ratio was maintained at the optimum ratio of ethanol:LA of 6:1 and SFC loading of 10 wt.%.

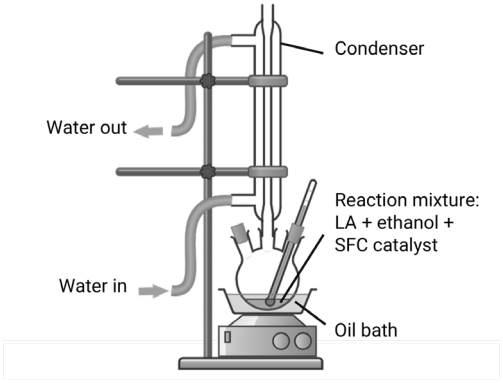


Figure 1 Experimental setup of LA conversion to EL

Gas chromatography-mass spectrometry was used to determine the concentrations of EL and LA. The analysis was conducted under the following conditions: 5MS column with temperature settings from 40 to 120 °C (3 °C/min), followed by from 120 to 280 °C (50 °C/min), and helium gas flow (1.0 mL/min). The calibration curves of standard concentrations of EL and LA were constructed to determine the chemical concentrations and calculate the yield and conversion accordingly. The yield and conversion were calculated using Eqs. (1) and (2) [19], respectively, as follows:

$$\text{EL Yield (mol\%)} = [(C_{EL} \times V_P)/1000/M_{EL}]/(M_{LA}/W_{LA}) \times 100\% \quad (1)$$

$$\text{LA conversion (\%)} = [W_{LA} - ((C_{LA} \times V_P)/1000)]/(W_{LA}) \times 100\% \quad (2)$$

Where C_{EL} and C_{LA} are the EL and LA concentrations (mg/L) in the final product, respectively; M_{EL} and V_{LA}

DOI: https://doi.org/10.11113/jurnalteknologi.v89.25102

are the molecular weights of EL (g/mol) and LA (g/mol), respectively; W_{LA} is the initial weight (g) of LA; and V_p is the volume of the final product (L).

2.3 Mathematical Equations for the Study of Reaction Kinetics and Thermodynamics

The chemical equation for the esterification of LA in ethanol to synthesise EL is shown in Eq. (3), while the equation for the reaction rate is presented in Eq. (4).

$$LA\ (C_A) + Ethanol\ (C_B) \leftrightarrow EL\ (C_C) + Water\ (C_D) \quad (3)$$

$$-r_A = -dC_A/dt = k_1 C_A^{\alpha} C_B^{\beta} - k_2 C_C^{\gamma} C_D^{\delta} \quad (4)$$

Where C is the concentration of the components, and the kinetic constants of k_1 and k_2 correspond to the forward and reverse reactions, respectively. Meanwhile, the α, β, γ, and δ represent their respective reaction order.

A similar kinetic model was adopted by Andreo-Martínez et al. [20], who used the following assumptions to determine the kinetic model equation for the LA esterification reaction:

1) The ethanol concentration can be considered constant as ethanol is the excess reactant.
2) The reaction is irreversible because an excess of ethanol is used, which drives the equilibrium reaction forward.

Therefore, the simplified kinetic model is as follows:

$$-dC_A/dt = k_1 C_A^{\alpha} C_B^{\beta} \quad (5)$$

$$-dC_A/dt = k C_A^{\alpha} \quad (6)$$

Where $k = k_1 C_B^{\beta}$ is a constant.

The integration method was used to solve the equation of the reaction order of LA. The experimental results were used to determine and justify the reaction kinetic order. According to Hoo and Abdullah [21], the reaction rate constant (k) and E_a for a heterogeneous catalyst are commonly investigated using a model equation of a simple power law. This study determined the k and E_a using the power-law model. The mathematical kinetic models of pseudo-zero, -first, and -second-order reactions were derived to explore the reaction order representing LA conversion based on the equation presented in Eq. (6). The integrated rate equations for the kinetic equations of pseudo-zero, -first, and -second-order kinetics are simplified in Eqs. (7), (8), and (9), respectively.

$$X_A C_{A0} = kt \quad (7)$$

$$\ln (1-X_A) = -kt \quad (8)$$

$$X_A/(1-X_A) = C_{A0}\, kt \quad (9)$$

Where X_A is the conversion of LA, k is the kinetic constant, t is the reaction time, and C_{A0} is the initial concentration of LA. The use of LA conversion in the kinetic study follows a similar approach to that of Zainol et al. [14].

Following the computation of the k values for pseudo-zero, first-, and second-order kinetic model equations, the k values of LA conversion were calculated from the slopes of the graphs of X_A, $\ln(1 - X_A)$, and $X_A/(1 - X_A)$ versus reaction time, respectively. In addition, the E_a and the reaction exponential factor (A) were determined from the plot of ln k versus 1/T obtained from the Arrhenius equation [14], as shown in Eq. (10).

$$\ln k = \ln A - E_a/RT \quad (10)$$

In the thermodynamic study, the Eyring and the activated complex equations were used to determine the thermodynamic activation parameters [14], as shown in Eqs. (11) and (12), respectively.

$$k = \frac{\kappa k_B T}{h} e^{-\frac{\Delta G^{++}}{RT}} \quad (11)$$

$$\Delta G^{++} = \Delta H^{++} - T\Delta S^{++} \quad (12)$$

The linearised Eyring equation was applied to calculate the thermodynamic activation parameters by plotting a ln k/T versus 1/T graph. Subsequently, Eq. (13) was used to determine ΔH and ΔS, while ΔG was calculated using Eq. (14).

$$\ln \frac{k}{T} = \frac{-\Delta H^{++}}{RT} + \ln \frac{k_B}{h} + \frac{\Delta S^{++}}{R} \quad (13)$$

$$\Delta G^{++} = -RT \ln \left(\frac{kh}{k_B T}\right) \quad (14)$$

Where ΔG^{++} refers to the Gibbs free energy of activation, ΔH^{++} represents the enthalpy of activation, ΔS^{++} refers to the entropy of activation at the state of the activated complex ($^{++}$), k is the rate constant, R is the gas constant, κ is the transmission factor assumed to be equal to 1, k_B is Boltzmann's constant (1.381×10^{23} J/K), h is Planck's constant (6.626×10^{-34} J·s), and T is the absolute temperature (K).

3.0 RESULTS AND DISCUSSION

3.1 Characteristics of the Catalyst

The peaks related to the functional groups of preheated char and sulfonated char catalyst in the wavelength range of 370–4000 cm^{-1} are shown in Figure 2. The spectra reveal a vibration band around 3000–3500 cm^{-1}, identified as O-H stretching. As stated by Nda-Umar et al. [22], the O-H stretching of the hydroxyl group is associated with phenols, carboxylic acids, or alcohols. The result explains that the O-H stretch is related to the sulfonated group attached to

DOI: https://doi.org/10.11113/jurnalteknologi.v89.25102

the catalyst structure and is possibly related to the physisorbed water on the catalyst structure. However, the O-H peak observed for the preheated char was not clearly shown, as the char was preheated at 200 °C, which removed the moisture of the char sample.

Similar to the sulfonated char catalyst, the heating at 200 °C was conducted after sulfonation to remove excess chemicals and moisture. Thus, the O-H of the sulfonated char is more related to the $–SO_3H$ groups attached to the catalyst structure. Peaks corresponding to S=O stretching and O=S=O stretching were observed in the sulfonated catalyst at 1091.78 and 847.46 $cm^{-1,}$ respectively [22, 23]. This confirms that the catalyst possesses $–SO_3H$ groups due to the covalent bonding between the $–SO_3H$ group and the carbon-based structure, providing an acidic active site for reaction [1, 24]. The C-H bond structure was observed around 2800–3000 cm^{-1} [22]. A small peak observed around the absorption band of 1400–1600 cm^{-1} is attributed to the C=C stretching of the aromatic compound, while the band between 1600 and 1750 cm^{-1} corresponds to C=O stretching [22, 25]. In addition, the presence of =C-H was detected in both preheated and sulfonated char at 903 cm^{-1} [23].

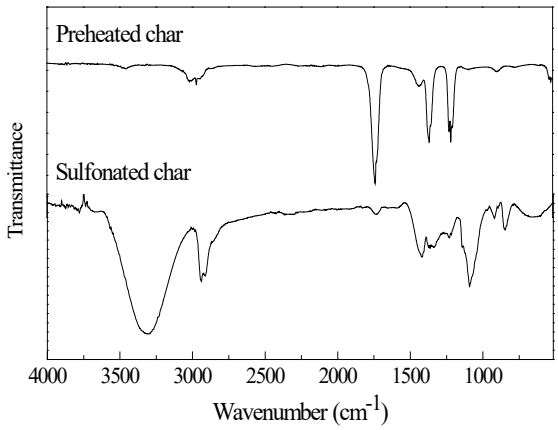


Figure 2 FTIR results for preheated char and sulfonated char

The results of the total surface area of the preheated char and sulfonated char catalyst are shown in Table 1. A low surface area of the sample was obtained due to the low temperature applied during the preheating of the char. The total surface area of the sulfonated char shows an increase attributable to the sulfonation process. However, there is no significant increase in the total surface area, as the thermal process involved in catalyst preparation is still at a low range of temperature (200 °C and below).

Table 1 Total surface area of preheated and sulfonated char

Sample	Surface area (m^2/g)
Preheated char	1.15
Sulfonated char	3.99

As reviewed by Ren et al. [26], the specific surface area of major chars derived from various biomass sources shows no significant change in surface area below 400 °C, which can be related to incomplete removal of volatiles. A significant change in surface area was observed at high temperatures above 400 °C, with the trend depending on the nature of the biomass used. In this work, a high surface area of the catalyst can be achieved if a high thermal heating process is applied to the modified catalyst surface, which may enhance the catalytic performance to synthesise a high yield of EL. However, further research is required to determine the optimal temperature for modification, as high temperatures will affect the degradation of functional groups that are important for the formation of active sites.

The thermal stability of the preheated char and sulfonated char is depicted by the TG/DTG curves shown in Figure 3. The TG curve is used to monitor changes in thermal stability, while the DTG curve indicates the degradation of possible components in the samples based on the observed peaks [25]. The first weight loss was observed from the TG curves of both preheated char and sulfonated char up to 150 °C. For the preheated char, a rapid weight reduction was observed up to 40 wt.% in the temperature range of 260–500 °C, and the weight of the preheated char continuously degraded up to 60 wt.% at 900 °C. As compared to sulfonated char, the TG curve shows a more stable structure, where low degradation was observed up to 400 °C, with approximately 90 wt.% of the sample remaining. Subsequently, the sample continuously decomposed up to 30 wt.% at 900 °C.

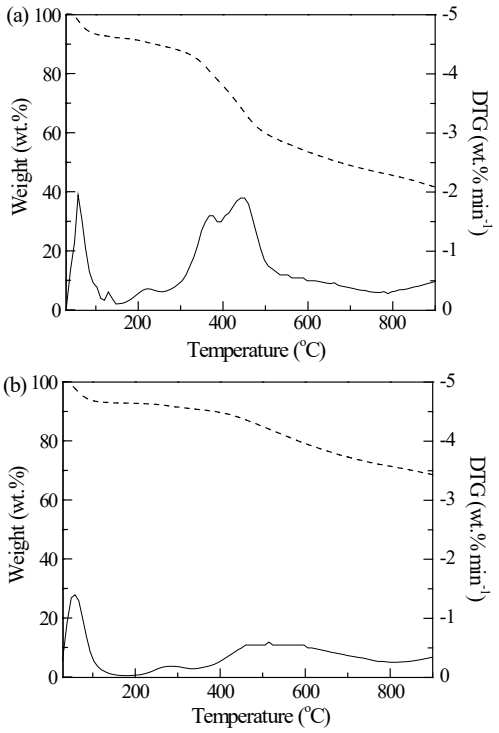


Figure 3 TG/DTG of (a) preheated and (b) sulfonated char

DOI: https://doi.org/10.11113/jurnalteknologi.v89.25102

Based on the DTG curves, high decomposition was observed in the preheated char (Figure 3(b)) between 200 and 500 °C. This is due to the major degradation of organic compounds in the char structure. Major degradation of the sample could occur above 200 °C as the char is produced via HTL at 225 °C, with the preheating process at 200 °C. The lower degradation rate observed from the DTG curve of the sulfonated char sample is affected by the sulfonation process conducted using concentrated H_2SO_4. However, further degradation was observed above 200 °C due to the loss of weight of the organic compound and decomposition of strong acid sites on the sulfonated char catalyst. According to Zainol et al. [25], the decomposition between 400 and 600 °C could be related to the decomposition of heavy organic compounds, including strong acid sites. Rocha et al. [27] stated that the weight loss observed in the range of 350–600 °C is due to the degradation of sulfonic groups, while Singare et al. [28] reported that 521 °C is the peak temperature related to the degradation of the sulfonate group.

The results in Table 2 show the elemental composition, such as C, H, N, S, and O, for preheated and sulfonated char. The preheated char and sulfonated char show a small difference in C content in their structure. This is because no carbon degradation occurs during sulfonation, and no thermal degradation occurs at higher temperatures during the process. However, the composition of the H element is reduced in the sulfonated char as compared to the precursor preheated char. This reduction results from the sulfonation process, which involves the attachment of sulfonate groups to the carbon structure of the aromatic ring.

Table 2 Elemental composition of preheated char and sulfonated char

Sample	Elemental composition (wt.%)				
	C	H	N	S	O[a]
Preheated char	44.51	27.66	3.95	0.28	23.60
Sulfonated char	44.01	14.28	3.85	0.91	36.95

[a] By difference

This statement can be related to the sulfonation process and the mechanism of carbon solid acid synthesis (via sulfonation), as explained by Zailan et al. [29]. Besides, the results are supported by the increasing number of S and O elements in the sulfonated char due to the introduction of the sulfonated group in the structure. The N element remained relatively unchanged, as it is not significantly involved in the sulfonation process. The N element is related to the component in the char of food waste, which can be related to the study by Mahssin et al. [12]. Based on the elemental composition obtained from the analysis and other characterisation techniques conducted, the results demonstrate the successful sulfonation process in preparing a solid acid catalyst from char.

3.2 Influence of Catalyst Particle Size and Agitation Speed on External and Internal Resistance

Figure 4(a) shows the results of LA conversion for different particle sizes at 2 and 4 h of reaction. The results indicate that the particle sizes considered in this study exhibit very small changes in conversion. However, conversion increased as the reaction time increased from 2 to 4 h. These specific particle sizes were selected for the kinetic study due to the small change in LA conversion, which neglects the effect of particle size on reaction performance. The reaction is kinetically controlled, which depends on the chemical reaction rate. Besides, the reaction rate is not limited by the movement of reactants (LA and ethanol) to the catalyst surface, as the available surface area of the catalyst remained sufficient for all tested particle sizes. Thus, the effect of particle size can be controlled in this study to mitigate its impact on the reaction rate. Similarly, Figure 4(b) illustrates that the agitation speeds studied had no significant influence on the conversion of LA. High agitation speed can potentially enhance the reaction by improving contact between the reactants and the catalyst, thereby increasing the reaction rate. However, within the range of agitation speed studied (100 and 300 rpm), no significant changes in conversion were observed. Therefore, the findings suggest that an average agitation speed of 200 rpm is suitable for further investigation in the reaction study.

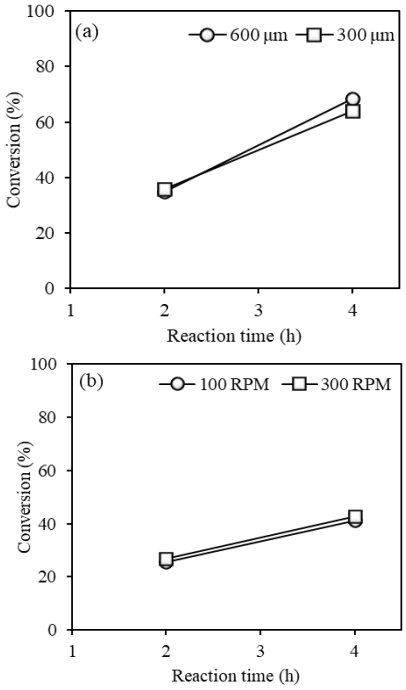


Figure 4 Reaction performance for different (a) particle sizes and (b) agitation speeds at different reaction times (at 10 wt.% SFC loading, 6:1 ethanol to LA, 80 °C)

DOI: https://doi.org/10.11113/jurnalteknologi.v89.25102

The influence of external and internal diffusion must be determined prior to conducting a study on reaction kinetics. The results are related to the mass transfer limitations that may occur from external and internal resistance, affecting the reaction rate of esterification [30]. The internal mass transfer is further discussed by investigating esterification using SFC particle sizes of 300 and 600 µm. Based on the results in Figure 4(a), there is negligible influence from internal mass transfer as the conversion shows minimal changes when these particle sizes were used for the reaction at 2 and 4 h. Similarly, the effect of agitation speed (Figure 4(b)) on LA conversion shows no significant impact when agitation speeds of 100 and 300 rpm were used. External mass transfer resistance could be eliminated by increasing the agitation speed, thereby improving contact between the reactants and the catalyst [31]. The lack of a clear effect on the reaction for the agitation speed applied indicates that the external mass transfer resistance can be neglected. Thus, the reaction is assumed to follow pseudo-homogeneous (P-H) reaction kinetics. The reaction kinetics were further investigated using the developed simple power-law kinetic model.

3.3 Influence of Reaction Time and Temperature on Conversion

The relationship between time and temperature in the LA esterification with ethanol was studied under fixed reaction conditions of 10 wt.% SFC, 6:1 ethanol to LA, 200 rpm agitation speed, and 300–600 µm particle size. As shown in Figure 5, the EL yield and LA conversion increased with longer reaction times and higher temperatures. Esterification at 80 °C exhibited the highest LA conversion and EL yield from 30 min to 4 h, with 16.90–68.36% and 16.87–68.36 mol%, respectively. This explains why esterification is typically conducted at reflux temperature. The yield and conversion were further observed at different reaction temperatures, and similar trends were observed for reactions at 60 and 70 °C. The yield and conversion increased as the temperature increased from 60 to 80 °C, indicating the significant influence of reaction temperature. A similar trend was observed by Sert [32].

For the esterification reaction at 60 °C, the conversion ranged from 6.00% to 23.02%, with the yield of 5.95–21.1 mol% over 30 min to 4 h. Meanwhile, at 70 °C, the esterification resulted in the conversion of 9.37–35.03%, with the yield of 8.48–33.45 mol% for the same period. As temperature increases, atoms tend to donate or receive electrons, which can further enhance the reaction activity [33]. A previous study on LA conversion to EL at temperatures of 60–120 °C reported that moderate conditions increased the reaction rate, although there was some reduction in yield at high temperatures [34]. A similar increase was observed for yield and conversion through the study of different reaction times. Increasing the reaction time allows more reactions to occur, leading to continuous production of EL.

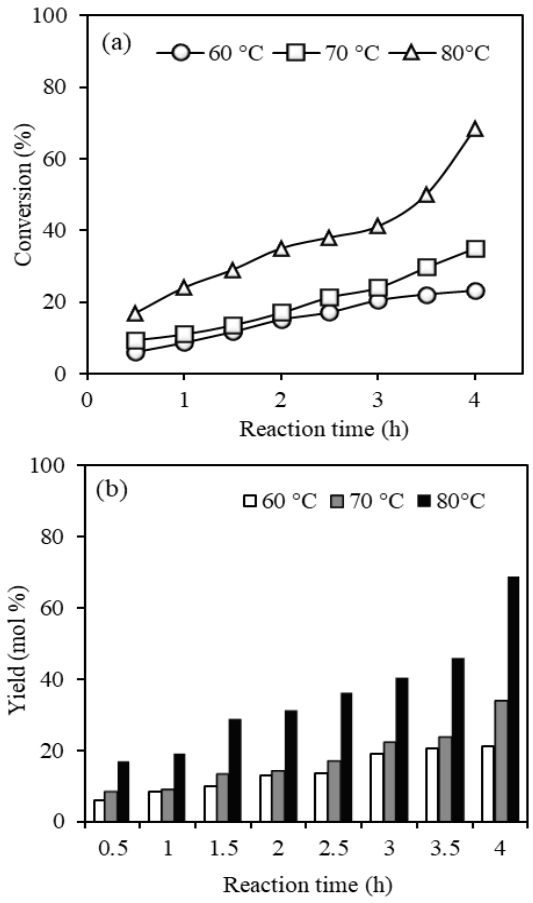


Figure 5 Influence of reaction time and temperature on (a) the conversion of LA and (b) the yield of EL (at 10 wt.% SFC, 6:1 ethanol to LA)

In this study, the reaction time was varied up to 4 h to further investigate the reaction kinetics. Typically, the yield increases as the reaction time approaches equilibrium; however, certain conditions may reduce the product yield due to side reactions during prolonged reactions. The presence of a catalyst in the reaction, along with the effect of reaction time and temperature, is important for achieving the optimum EL yield [15, 35]. A high yield of EL at 80 °C indicates effective catalyst activity compared to the results at 60 and 70 °C. Importantly, the carbon catalyst accelerates the esterification reaction, leading to a higher product yield compared to reactions without a catalyst, as reported by Fernandes et al. [36]. Without a catalyst, they achieved only 2% conversion of LA after 5 h of reaction at 70 °C.

3.4 Kinetic Study

In Figure 6(a), the pseudo-zero-order linear plot shows a good fit to the experimental data at reaction temperatures of 60, 70, and 80 °C. However, the pseudo-first-order linear plot has a better fit to the experimental data at 60 and 70 °C, with a poorer fit at 80 °C, as displayed in Figure 6(b). In Figure 6(c), the

DOI: https://doi.org/10.11113/jurnalteknologi.v89.25102

pseudo-second-order linear plot exhibits high deviation from the experimental data for the reaction temperature of 80 °C. The coefficients of determination (R^2) for all kinetic models are listed in Table 3. The linear graph of the pseudo-first-order models is satisfactory, with high R^2 values close to one. This shows that pseudo-first-order models are the best fit for the reaction, as further supported by previous studies reported by Zainol et al. [15], Yadav and Yadav [17] Consequently, this model was selected for the esterification of LA to EL using the SFC catalyst. The values of k for the pseudo-first-order kinetic models at 60, 70, and 80 °C are listed in Table 3.

Table 3 Parameters of P-H kinetic models for LA conversion to EL using the SFC catalyst

Temp. (°C)	Regression coefficient (R^2)			First-order, k (min^{-1})
	Zero-order	First-order	Second-order	
60	0.9863	0.9911	0.9947	0.0012
70	0.9907	0.9914	0.9865	0.0017
80	0.9787	0.9606	0.8795	0.0038

The kinetic results of this study can be used to explain the reaction mechanism. The esterification follows a proton-catalysed route, where the reaction rate depends mainly on the LA concentration. Specifically, the mechanism steps involve the activation of LA by the acid sites of the SFC catalyst, followed by nucleophilic attack by ethanol. Table 4 presents the A and E_a values using the SFC catalyst. The Arrhenius constant and E_a values were determined from the intercept and slope of the plot in Figure 6(a), respectively. Activation energy represents the minimum energy needed for the reaction to occur, and is related to the catalytic activity of the SFC catalyst. The obtained E_a value of 56.1 kJ/mol (based on the P-H first-order model) exceeds the 15 kJ/mol threshold [14].

Table 4 Exponential factor (A) and E_a of LA conversion to EL using SFC catalyst

Reaction Conditions	R^2	A (min^{-1})	E_a (kJ/mol)
60–80 °C SFC catalyst	0.9428	2.60	56.1

The obtained E_a value suggests that the catalyst effectively lowers the energy barrier, thereby enhancing the reaction rate for the conversion of LA. Additionally, this implies that the reaction depends on the catalyst's activity and reaction kinetics, rather than on mass transfer [37]. Kokare et al. [35] reported E_a values of 34.91 and 39.89 kJ/mol using Amberlyst-15. Nandiwale et al. [30] found that the esterification using desilicated HZSM-5 catalyst achieved an E_a of 21.1 kJ/mol. The E_a values from previous studies employing different catalysts and reaction conditions are presented in Table 5.

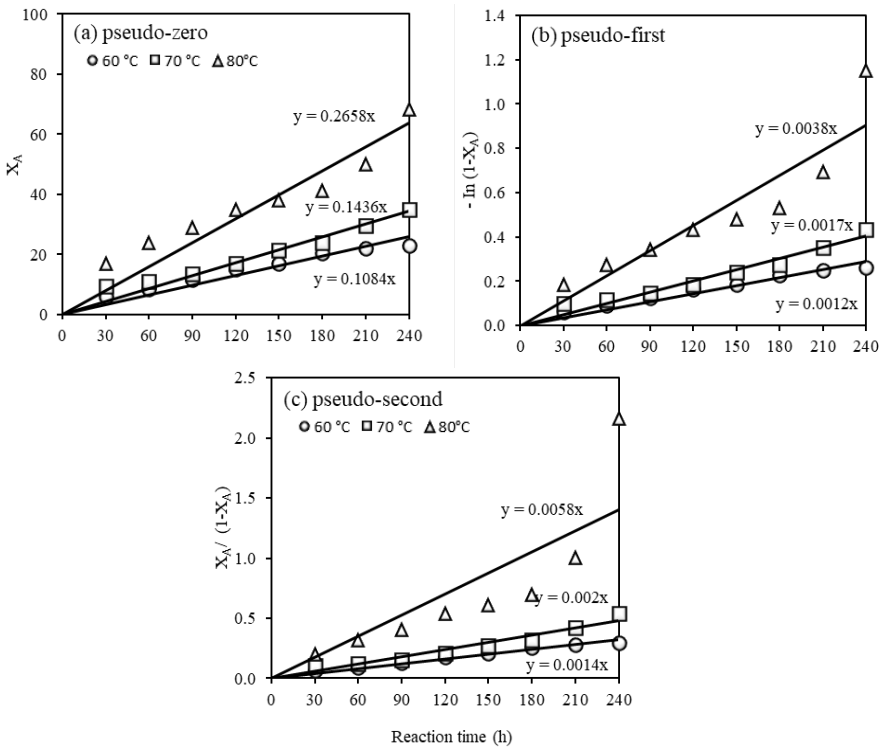


Figure 6. Plots of P-H kinetic models for LA conversion

DOI: https://doi.org/10.11113/jurnalteknologi.v89.25102

Most kinetic studies utilised the P-H kinetic model to determine the kinetic parameters. Comparing the E_a values, the SFC catalyst is considered to have lower catalytic activity due to its high E_a of 56.1 kJ/mol. Previous research has indicated that modified zeolite catalysts exhibited good catalytic activity, with E_a values ranging from 20 to 30 kJ/mol for EL synthesis [5, 30]. Nandiwale and Bokade [38] studied the esterification reaction with different types of alcohols with micro/meso HZ-5 catalyst and obtained varying E_a values for each alcohol employed. For the esterification of LA with ethanol, the micro/meso HZ-5 catalyst was reported to have an E_a of 27.4 kJ/mol. The E_a obtained for the SFC catalyst is higher than that reported for other catalysts, which can be attributed to the low catalytic activity of the SFC catalyst. This difference may be influenced by catalyst properties, such as the number and strength of acid sites. Nevertheless, the properties of the SFC catalyst could be improved through catalyst modification in future studies.

Table 5 Selected reaction kinetic models and corresponding E_a for various catalysts in previous studies

Catalyst	Reaction Conditions	Kinetic Model	E_a (kJ/mol)	Ref.
Amberlyst-15	87–127 °C (n-Butanol)	P-H	34.91	(Kokare et al., 2018)
Amberlyst-15	87–127 °C (n-Butanol)	L-H	39.89	(Kokare et al., 2018)
Desilicated HZSM-5	90–130 °C (Ethanol)	P-H	21.1	(Nandiwale et al., 2014)
DPTA/DH-ZSM-5	76–84 °C (Ethanol)	P-H	29.4	(Nandiwale et al., 2013)
Micro/meso HZ-5	90–130 °C (Ethanol)	P-H	27.4	(Nandiwale & Bokade, 2015)
Micro/meso HZ-5	90–130 °C (Methanol)	P-H	51.6	(Nandiwale & Bokade, 2015)
SFC catalyst	60–80 °C (Ethanol)	P-H	56.1	This work

3.5 Thermodynamic Study

Figure 7 shows the plot used to determine the thermodynamic parameters of the reaction, while Table 6 summarises the thermodynamic parameters obtained in this study. The enthalpy value obtained is 53.2 kJ/mol, which is higher than that reported by Zainol et al. [15], who used a carbon cryogel catalyst and obtained a lower enthalpy of activation of 17 kJ/mol. This suggests that the process using the SFC catalyst is more endothermic and requires more heat to form EL. In addition, the entropy of activation is -190.9 J/mol·K, indicating that the system is less disordered. Moreover, the Gibbs free energy of activation is 84.4 kJ/mol, suggesting an endergonic reaction, which explains why the reaction is not spontaneous. A previous study by Tiong et al. [16] reported an enthalpy of activation of 25.1 kJ/mol·K, an entropy of activation of -172.4 J/mol·K, and a Gibbs free energy of activation of 90.3 kJ/mol.

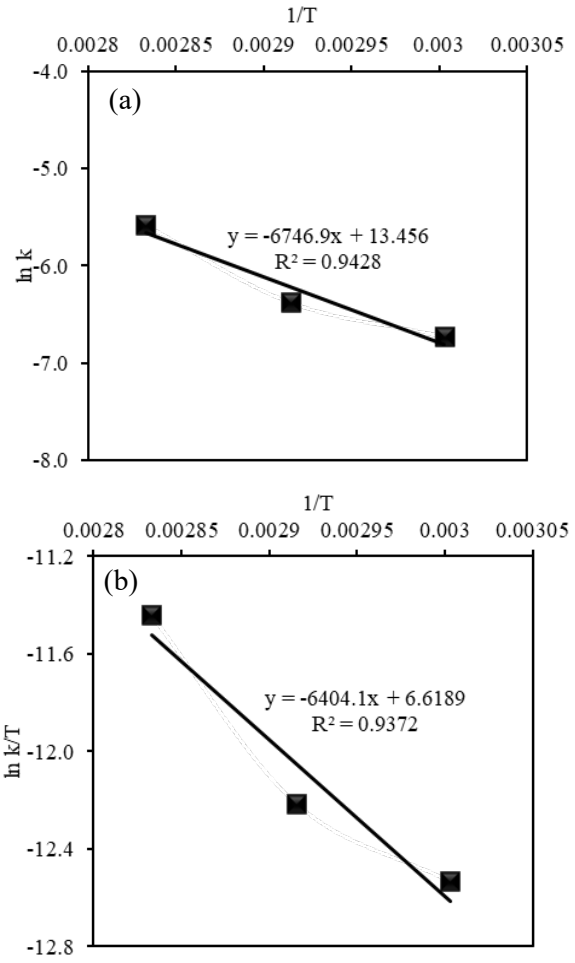


Figure 7 Plots of (a) ln k against 1/T and (b) ln k/T against 1/T for LA esterification catalysed by SFC

These thermodynamic parameters are consistent with the current study, except for the enthalpy of activation, which is more than double the value reported in the previous study. The high enthalpy of activation is supported by the high E_a observed in this study, indicating low catalytic activity.

Table 6 Thermodynamic parameters of LA conversion to EL catalysed by the SFC catalyst

Reaction Conditions	R^2	ΔH^{++} (kJ/mol)	ΔS^{++} (J/mol·K)	ΔG^{++} (kJ/mol)
60–80 °C SFC catalyst	0.9372	53.2	-190.9	84.4

The kinetic parameters are important for determining the thermodynamic parameters for the reaction conducted using the developed simple power-law kinetic model. This kinetic model is commonly used to investigate reactions involving homogeneous

DOI: https://doi.org/10.11113/jurnalteknologi.v89.25102

catalysts and has also been applied to heterogeneous catalyst reactions. The obtained kinetic and thermodynamic parameters will be valuable for future simulation work and process scale-up. Further research could explore the determination of kinetic parameters using other kinetic models, such as diffusion models and/or mechanism-based kinetic models (e.g., Langmuir-Hinshelwood and Eley-Rideal mechanisms). This proposed work may lead to the development of more advanced kinetic models that can enhance the output of simulation studies and reactor design.

4.0 CONCLUSION

The esterification of LA catalysed by SFC occurs within the kinetic range, as indicated by the investigation of the effect of diffusion. This study developed kinetic models for LA conversion to EL, and among these models, the pseudo-first-order model best describes the reaction. The E_a of LA esterification using the SFC catalyst is 56.1 kJ/mol. Utilising the Eyring equation for thermodynamic parameter evaluation, the results suggest that the system at the transition state for EL synthesis is more organised because the reaction is endergonic rather than spontaneous. Due to the high E_a values obtained in the esterification reaction using SFC, it is recommended to enhance the catalyst through modification to increase catalytic activity and lower the E_a of the reaction. Future studies may explore diffusion models and/or mechanism-based kinetic models to improve outcomes and determine the significant kinetic models suitable for representing the reaction process in simulation studies and scale-up.

Acknowledgement

The authors would like to express their gratitude to the Ministry of Higher Education (MOHE), Malaysia for the financial support through the Fundamental Research Grant Scheme (FRGS/1/2021/TK0/UITM/02/7), and to the College of Engineering, Universiti Teknologi MARA (UiTM) for providing the facilities necessary to conduct this research.

Conflicts of Interest

The authors declare that there is no conflict of interest regarding the publication of this paper.

Data availability

The data supporting the findings of this study are available from the corresponding author upon reasonable request.

Ethics declaration

Formal ethical approval was not obtained for this study. However, the authors confirm that the research was conducted in accordance with established ethical principles and good research practices, with due consideration given to participant rights, informed consent, confidentiality, and responsible data handling.

References

[1] Badgujar, K.C., Badgujar, V.C., Bhanage, B.M. (2020). A review on catalytic synthesis of energy rich fuel additive levulinate compounds from biomass derived levulinic acid. *Fuel Processing Technology*. 197, 106213. DOI: https://doi.org/10.1016/j.fuproc.2019.106213.

[2] Oprescu, E.-E., Enascuta, C.-E., Doukeh, R., Calin, C., Lavric, V. (2021). Characterizing and using a new bi-functional catalyst to sustainably synthesize methyl levulinate from biomass carbohydrates. *Renewable Energy*. 176, 651-662. DOI: https://doi.org/10.1016/j.renene.2021.05.120.

[3] [3] Démolis, A., Essayem, N., Rataboul, F. (2014). Synthesis and applications of alkyl levulinates. *ACS Sustainable Chemistry & Engineering*. 2, 1338-1352. DOI: https://doi.org/10.1021/sc500082n.

[4] Ramli, N.A.S., Hisham, N.I., Amin, N.A.S. (2018). Esterification of levulinic acid to levulinate esters in the presence of sulfated silica catalyst. *Sains Malaysiana*. 47, 1131-1138. DOI: http://dx.doi.org/10.17576/jsm-2018-4706-08.

[5] Nandiwale, K.Y., Sonar, S.K., Niphadkar, P.S., Joshi, P.N., Deshpande, S.S., Patil, V.S., Bokade, V.V. (2013). Catalytic upgrading of renewable levulinic acid to ethyl levulinate biodiesel using dodecatungstophosphoric acid supported on desilicated H-ZSM-5 as catalyst. *Applied Catalysis A: General*. 460, 90-98. DOI: https://doi.org/10.1016/j.apcata.2013.04.024.

[6] Peng, L., Li, H., Xi, L., Chen, K., Chen, H. (2014). Facile and efficient conversion of furfuryl alcohol into n-butyl levulinate catalyzed by extremely low acid concentration. *BioResources*. 9, 3825-3834. DOI: https://doi.org/10.15376/biores.9.3.3825-3834.

[7] Gupta, P., Paul, S. (2014). Solid acids: Green alternatives for acid catalysis. *Catalysis Today*. 236, 153-170. DOI: https://doi.org/10.1016/j.cattod.2014.04.010.

[8] Bakhtiari, B., Najafi Chermahini, A., Babaei, Z. (2021). Design of an acidic sulfonated mesoporous carbon catalyst for the synthesis of butyl levulinate from levulinic acid. *Environmental Progress & Sustainable Energy*. 40, e13721. DOI: https://doi.org/10.1002/ep.13721.

[9] Guo, H., Hirosaki, Y., Qi, X., Smith Jr, R.L. (2020). Synthesis of ethyl levulinate over amino-sulfonated functional carbon materials. *Renewable Energy*. 157, 951-958. DOI: https://doi.org/10.1016/j.renene.2020.05.103.

[10] Kitano, M., Arai, K., Kodama, A., Kousaka, T., Nakajima, K., Hayashi, S., Hara, M. (2009). Preparation of a sulfonated porous carbon catalyst with high specific surface area. *Catalysis letters*. 131, 242-249. DOI: https://doi.org/10.1007/s10562-009-0062-4.

[11] Hassan, A.H., Zainol, M.M., Samion, M.A., Azlan, M.A.q., Asmadi, M., Mohamad Daud, A.R., Saad, I., Mohd Nor Azman, N.A.N. (2023). Synthesis of ethyl levulinate over sulfonated lignin-based carbon catalyst as a fuel additive to biodiesel-diesel blends towards engine emissions. *Journal of Cleaner Production*. 418, 138101. DOI: https://doi.org/10.1016/j.jclepro.2023.138101.

[12] Mahssin, Z.Y., Zainol, M.M., Hassan, N.A., Yaacob, H., Puteh, M.H., Amin, N.A.S. (2021). Hydrothermal liquefaction

bioproduct of food waste conversion as an alternative composite of asphalt binder. *Journal of Cleaner Production*. 282, 125422. DOI: https://doi.org/10.1016/j.jclepro.2020.125422.
[13] Kajdas, C., Kulczycki, A., Kurzydłowski, K., Molina, G.J. (2010). Activation energy of tribochemical and heterogeneous catalytic reactions. *Materials Science-Poland*. 28, 523-533.
[14] Zainol, M.M., Asmadi, M., Amin, N.A.S. (2022). Bio-fuel additive synthesized from levulinic acid using ionic liquid-furfural based carbon catalyst: Kinetic, thermodynamic and mechanism studies. *Chemical Engineering Science*. 247, 117079. DOI: https://doi.org/10.1016/j.ces.2021.117079.
[15] Zainol, M.M., Amin, N.A.S., Asmadi, M. (2019). Kinetics and thermodynamic analysis of levulinic acid esterification using lignin-furfural carbon cryogel catalyst. *Renewable Energy*. 130, 547-557. DOI: https://doi.org/10.1016/j.renene.2018.06.085.
[16] Tiong, Y.W., Yap, C.L., Gan, S., Yap, W.S.P. (2020). Kinetic and thermodynamic studies of oil palm mesocarp fiber cellulose conversion to levulinic acid and upgrading to ethyl levulinate via indium trichloride-ionic liquids. *Renewable Energy*. 146, 932-943. DOI: https://doi.org/10.1016/j.renene.2019.07.024.
[17] Yadav, G.D., Yadav, A.R. (2014). Synthesis of ethyl levulinate as fuel additives using heterogeneous solid superacidic catalysts: Efficacy and kinetic modeling. *Chemical Engineering Journal*. 243, 556-563. DOI: https://doi.org/10.1016/j.cej.2014.01.013.
[18] Hassan, A.H., Zainol, M.M., Zainuddin, K.R., Saperi, N.Q., Yussuf, M.A.M., Abd Rahman, N., Azman, N.A.N.M.N. (2022). Sulfonated Carbon Catalyst Prepared from Calcination of Lignin for Ethyl Levulinate Synthesis via Ethanolysis of Levulinic Acid. *Chemical Engineering Transactions*. 97, 307-312. DOI: https://doi.org/10.3303/CET2297052.
[19] Hassan, A.H., Zainol, M.M., Samion, M.A., Asmadi, M., Daud, A.R.M., Saad, I., Azman, N.A.N.M.N. (2023). Synthesis of ethyl levulinate over sulfonated lignin-based carbon catalyst as a fuel additive to biodiesel-diesel blends towards engine emissions. *Journal of Cleaner Production*. 418, 138101. DOI: https://doi.org/10.1016/j.jclepro.2023.138101
[20] Andreo-Martínez, P., García-Martínez, N., del Mar Durán-del-Amor, M., Quesada-Medina, J. (2018). Advances on kinetics and thermodynamics of non-catalytic supercritical methanol transesterification of some vegetable oils to biodiesel. *Energy Conversion and Management*. 173, 187-196. DOI: https://doi.org/10.1016/j.enconman.2018.07.069
[21] Hoo, P., Abdullah, A.Z. (2015). Kinetics modeling and mechanism study for selective esterification of glycerol with lauric acid using 12-tungstophosphoric acid post-impregnated SBA-15. *Industrial & Engineering Chemistry Research*. 54, 7852-7858. DOI: https://doi.org/10.1021/acs.iecr.5b02304.
[22] Nda-Umar, U.I., Ramli, I., Muhamad, E.N., Taufiq-Yap, Y.H., Azri, N. (2020). Synthesis and characterization of sulfonated carbon catalysts derived from biomass waste and its evaluation in glycerol acetylation. *Biomass Conversion and Biorefinery*. 1-16. DOI: https://doi.org/10.1007/s13399-020-00784-0.
[23] Kastner, J., R., Miller, J., Geller, D.P., Locklin, J., Keith, L.H., Johnson, T. (2012). Catalytic esterification of fatty acids using solid acid catalysts generated from biochar and activated carbon. *Catalysis Today*. 190, 122-132. DOI: https://doi.org/10.1016/j.cattod.2012.02.006.
[24] Hara, M. (2010). Biodiesel Production by Amorphous Carbon Bearing SO_3H, COOH and Phenolic OH Groups, a Solid Brønsted Acid Catalyst. *Topics in Catalysis*. 53, 805-810. DOI: https://doi.org/10.1007/s11244-010-9458-z
[25] Zainol, M.M., Asmadi, M., Iskandar, P., Wan Ahmad, W.A.N., Amin, N.A.S., Hoe, T.T. (2021). Ethyl levulinate synthesis from biomass derivative chemicals using iron doped sulfonated carbon cryogel catalyst. *Journal of Cleaner Production*. 281, 124686. DOI: https://doi.org/10.1016/j.jclepro.2020.124686.
[26] Ren, J., Cao, J.-P., Zhao, X.-Y., Liu, Y.-L. (2021). Fundamentals and applications of char in biomass tar reforming. *Fuel Processing Technology*. 216, 106782. DOI: https://doi.org/10.1016/j.fuproc.2021.106782.
[27] Rocha, P.D., Oliveira, L.S., Franca, A.S. (2019). Sulfonated activated carbon from corn cobs as heterogeneous catalysts for biodiesel production using microwave-assisted transesterification. *Renewable Energy*. 143, 1710-1716. DOI: https://doi.org/10.1016/j.renene.2019.05.070.
[28] Singare, P.U., Lokhande, R.S., Madyal, R.S. (2011). Thermal degradation studies of some strongly acidic ca-tion exchange resins. *Open Journal of Physical Chemistry*. 1, 45. DOI: https://doi.org/10.4236/ojpc.2011.12007.
[29] Zailan, Z., Tahir, M., Jusoh, M., Zakaria, Z.Y. (2021). A review of sulfonic group bearing porous carbon catalyst for biodiesel production. *Renewable Energy*. 175, 430-452. DOI: https://doi.org/10.1016/j.renene.2021.05.030.
[30] Nandiwale, K.Y., Niphadkar, P.S., Deshpande, S.S., Bokade, V.V. (2014). Esterification of renewable levulinic acid to ethyl levulinate biodiesel catalyzed by highly active and reusable desilicated H-ZSM-5. *Journal of Chemical Technology & Biotechnology*. 89, 1507-1515. DOI: https://doi.org/10.1002/jctb.4228.
[31] Ramli, N.A.S., Amin, N.A.S. (2016). Kinetic study of glucose conversion to levulinic acid over Fe/HY zeolite catalyst. *Chemical Engineering Journal*. 283, 150-159. DOI: https://doi.org/10.1016/j.cej.2015.07.044.
[32] Sert, M. (2020). Catalytic effect of acidic deep eutectic solvents for the conversion of levulinic acid to ethyl levulinate. *Renewable Energy*. 153, 1155-1162. DOI: https://doi.org/10.1016/j.renene.2020.02.070.
[33] Tian, L., Zhang, L., Liu, Y., He, Y., Zhu, Y., Sun, R., Yi, S., Xiang, J. (2020). Clean production of ethyl levulinate from kitchen waste. *Journal of Cleaner Production*. 268, 122296. DOI: https://doi.org/10.1016/j.jclepro.2020.122296.
[34] Mthembu, L., Lokhat, D., Deenadayalu, N. (2021). Esterification of levulinic acid to ethyl levulinate: optimization of process conditions using commercial levulinic acid and extension to the use of levulinic acid derived from depithed sugarcane bagasse. *Biomass Conversion and Biorefinery*. 1-10. DOI: https://doi.org/10.1007/s13399-021-01632-5.
[35] Kokare, M.B., Ranjani, V., Mathpati, C. (2018). Response surface optimization, kinetic study and process design of n-butyl levulinate synthesis. *Chemical Engineering Research and Design*. 137, 577-588. DOI: https://doi.org/10.1016/j.cherd.2018.07.036.
[36] Fernandes, D., Rocha, A., Mai, E., Mota, C.J., Da Silva, V.T. (2012). Levulinic acid esterification with ethanol to ethyl levulinate production over solid acid catalysts. *Applied Catalysis A: General*. 425, 199-204. DOI: https://doi.org/10.1016/j.apcata.2012.03.020.
[37] Dhawane, S.H., Al-Sakkari, E., Kumar, T., Halder, G. (2021). Comprehensive elucidation of the apparent kinetics and mass transfer resistances for biodiesel production via in-house developed carbonaceous catalyst. *Chemical Engineering Research and Design*. 165, 192-206. DOI: https://doi.org/10.1016/j.cherd.2020.11.003
[38] Nandiwale, K.Y., Bokade, V.V. (2015). Environmentally benign catalytic process for esterification of renewable levulinic acid to various alkyl levulinates biodiesel. *Environmental Progress & Sustainable Energy*. 34, 795-801. DOI: https://doi.org/10.1002/ep.12042.